Collisional effects on global gyrokinetic particle-in-cell simulations of ITG and TEM instabilities in tokamaks

K. Kauffmann[1], R. Kleiber[1], R. Hatzky[2]

[1] *Max Planck Institut für Plasmaphysik, D-17491, Greifswald, Germany*

[2] *Max Planck Institut für Plasmaphysik, D-85748, Garching, Germany*

Particle and heat transport in tokamaks exceed the neoclassical prediction. This anomalous transport is produced by turbulence which is probably caused by microinstabilities such as ion and electron-temperature-gradient (ITG/ETG) and trapped-electron-mode (TEM). This work studies the effects of collisions on these instabilities by using the 3D global gyrokinetic PIC code EUTERPE. In this code, the distribution function of each species evolves according to the set of gyrokinetic equations,

$$\frac{df}{dt} = \frac{\partial f}{\partial t} + \dot{\mathbf{R}}\frac{\partial f}{\partial \mathbf{R}} + \dot{v}_{\|}\frac{\partial f}{\partial v_{\|}} = C(f) \tag{1}$$

where $C(f)$ is a collision operator, for example the Fokker-Planck operator. The guiding center trajectories (characteristics) for the collisionless case are:

$$\dot{\mathbf{R}} = v_{\|}\hat{\mathbf{b}} + \frac{1}{B^*}\left(\frac{\mu B + v_{\|}^2}{\Omega_{\mathrm{i}}}\hat{\mathbf{b}}\times\nabla B + \frac{v_{\|}^2}{\Omega_{\mathrm{i}}}(\nabla\times\mathbf{B})_{\perp}\right) \tag{2}$$

$$\dot{v}_{\|} = -\mu\left(\hat{\mathbf{b}} + \frac{v_{\|}}{B^*\Omega_{\mathrm{i}}}(\nabla\times\mathbf{B})_{\perp}\right)\cdot\nabla B \tag{3}$$

where $\mu \overset{\mathrm{def}}{=} \frac{v_{\perp}^2}{2B}$, $\hat{\mathbf{b}} \overset{\mathrm{def}}{=} \frac{\mathbf{B}}{B}$ and $B^* \overset{\mathrm{def}}{=} B + \frac{m_{\mathrm{i}}v_{\|}}{q_{\mathrm{i}}}\hat{\mathbf{b}}\cdot(\nabla\times\hat{\mathbf{b}})$. Quasineutrality closes the system

$$-\nabla_{\perp}\cdot\left(\frac{m_i n_0}{q_i B^2}\nabla_{\perp}\phi\right) + \frac{e n_0}{k_B T}\phi = \langle n_i\rangle = \int f(\vec{R}, v_{\|}, \mu)\delta(\vec{R}+\vec{\rho}-\vec{x})d\vec{R}d\vec{v}\,. \tag{4}$$

The code utilizes the δf method [1] in which, for each species, the distribution function is divided into a background equilibrium distribution function and a perturbed part $f = f_0 + \delta f$. This makes it possible to compute only the time evolution of the perturbation, which reduces the statistical noise as compared with the full-f method. Since EUTERPE has been extended to include collisions and multiple species, a generalized collisional δf scheme was implemented. This is known as the two-weight scheme [2, 3, 4]: with collisions, the weight evolution of the Monte-Carlo markers cannot be solved directly by the method of characteristics, because the diffusive particle motion causes the "characteristic line", along which the convective derivative

of the weight is to be evaluated, to be stochastic. To overcome this problem, it is better not to define the weight in terms of the local δf, but to treat the weight as another variable, in addition to the usual dimensions of $x-v$ space. By taking the moments of the new kinetic equation in the extended phase space, it is possible to choose the weights to be consistent with the original δf equation. By doing so, one finds that the evaluation of the marker density becomes difficult, unless a second weight is added to the extended phase space. In the cases we have studied, however, ($C(f_0)=0$ and zeroth order of $df_0/dt=0$) the second weight does not evolve, which is equivalent to having a one-weight scheme.

The collisions are modelled by the pitch angle scattering operator $C_a(f_a)=\nu_a\mathscr{L}(f_a)$, where a denotes the species, and $\mathscr{L}$ is the Lorentz operator. In the code, the collisionality is implemented by modifying the trajectories in velocity space, introducing two random numbers, which correspond to the spherical angles. This means that particles diffuse on a spherical shell in velocity space, but do not change the magnitude of the velocity, thus conserving energy. It is important to point out that this operator does not conserve momentum, but the scheme could be extended to comply with that requirement if needed.

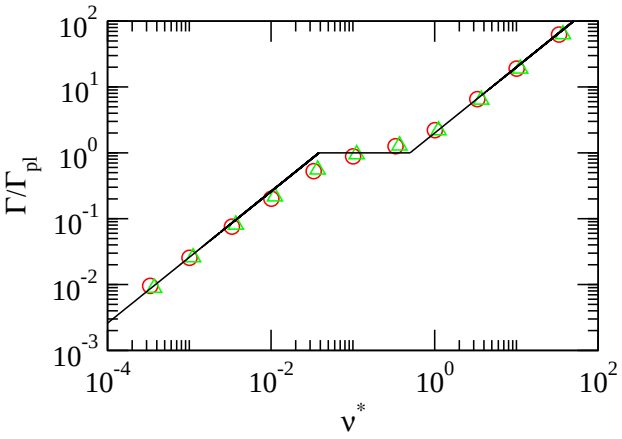

Figure 1: *Neoclassical radial particle flux at $s=0.5$ for a tokamak of aspect ratio $A=5$ obtained with EUTERPE (red), DKES (green) and the analytical values (black). The flux is normalized to the analytical flux in the plateau regime and the collision frequency is normalized to the bounce frequency.*

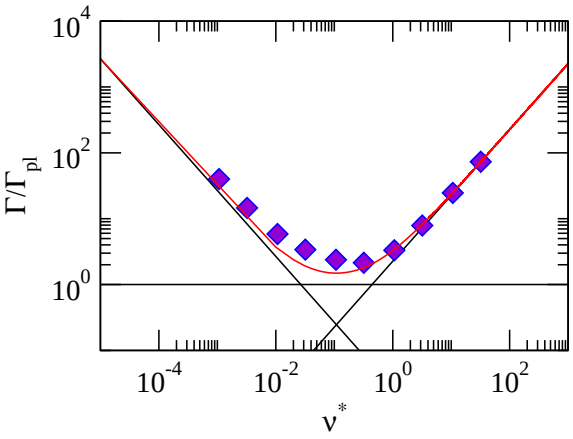

Figure 2: *Neoclassical radial particle flux at $s=0.5$ for the LHD stellarator with the "standard" magnetic configuration for $R=3.75$ m with no radial electric field $E_r=0$ Results shown for EUTERPE (violet) and the analytical values (black). The red line is the sum of the analytical results for the different collisionality regimes.*

As a benchmark, the neoclassical radial particle flux was calculated and compared with the analytical calculations, as well as with the Drift Kinetic Equation Solver (DKES) code [5] as shown in Fig. 1. For these comparisons, all the particles were loaded on one flux-surface ($s=0.5$) and

for simplicity, only a radial density gradient was considered (no temperature gradients). Also, to avoid the particles leaving the flux-surface, the radial spatial drifts were artificially suppressed, but retained as driving terms in the evolution of the distribution. It is of relevance to note that the particles are not monoenergetic, therefore it is necessary to perform the convolution over the results in order to compare with the monoenergetic DKES.

A benchmark was also performed for the case of a stellarator with no radial electric field ($E_r = 0$) as shown in Fig. 2. The equilibrium configuration is the magnetic geometry given by the "standard" LHD case with $R = 3.75$ m. As the figure shows, EUTERPE is in good agreement with the analytical results. For each point in the graph, the flux was calculated in time, until it saturated and this value was taken as a data point. Both for the tokamak and stellarator case, it is important to let the simulation run at least two or more collision times, which is especially time consuming when the collisionality is small, since the time step cannot be larger than a certain limit imposed by numerical stability.

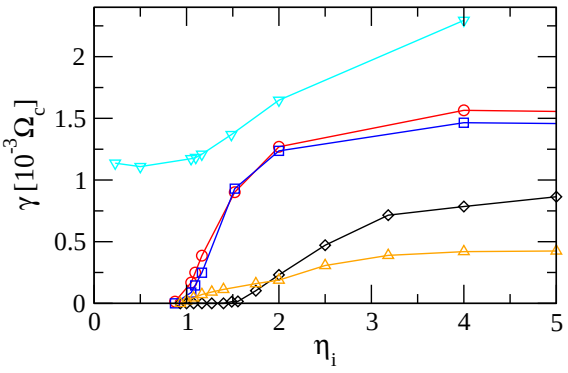

Figure 3: *Growth rate vs. η_i. The parameters used were: aspect ratio $A = 3$ and for the collisional cases $\nu = 0.01\Omega_c$. Slab ITG's: collisional (orange), no collisions (black). Toroidal ITG's: collisional (red), no collisions (blue). Simulations with kinetic electrons are depicted in cyan.*

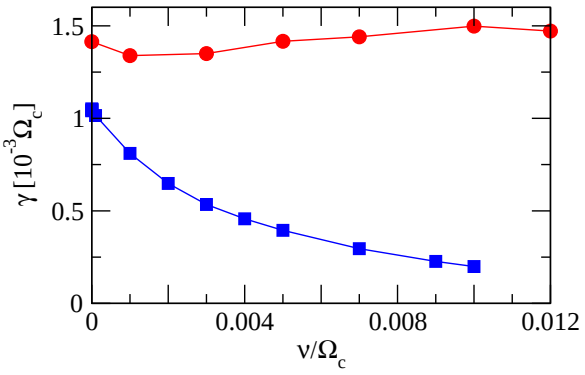

Figure 4: *Growth rate dependence on collisionality for high η_i. In red is the toroidal ITG mode and in blue is the slab ITG mode. It is possible to observe that collisions do not significantly alter the toroidal ITG.*

With collisions now implemented, it is possible to investigate their effect on instabilities. At first, a cylindrical geometry with adiabatic electrons was considered. To observe the η_i threshold for the slab ITG modes the κ_T profile was changed while leaving the κ_n profile without variations (where $\kappa_T = -\nabla \ln T$ and $\kappa_n = -\nabla \ln n$). This was first performed without collisions and then again using a high collision frequency ($\nu = 0.01\Omega_c$). The same procedure was applied when studying the tokamak configuration with adiabatic electrons. For the study of TEM instabilities in a tokamak, fully kinetic ions and electrons were used. The results can bee seen in

Fig. 3. One can observe that the instability threshold value of $\eta_i = \kappa_T/\kappa_n$ in a slab magnetic geometry (for $k_\perp \rho_i \ll 1$) is reduced by collisions. This is due to the coupling between parallel and perpendicular temperatures [6]. In the "collisionless" plasma limit, there is no coupling, thus the threshold is higher. In the opposite case, where the plasma is highly collisional, the threshold drops as a consequence of the additional degrees of freedom of the system. Now the parallel and perpendicular temperatures are strongly coupled. A strong dependence of the growth rate on collisionality can be observed in Fig. 4.

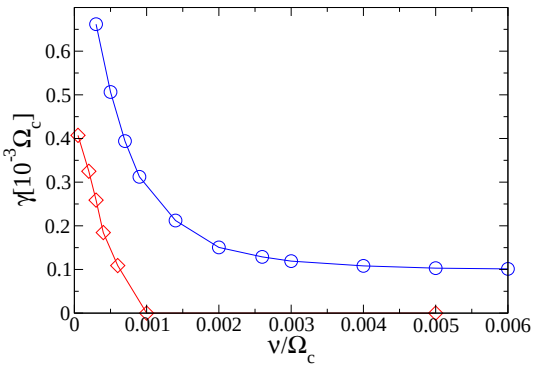

Figure 5: *TEM instability growth rate as a function of collisionality for* $R/L_{Te} = 0$, $R/L_{Ti} = 3.21$. *Blue circles represent the values for* $R/L_n = 3.75$. *Red diamonds, for* $R/L_n = 2.57$

For toroidal ITG modes, however, collisionality does not have a significant effect (see Fig. 4), which is in agreement with theoretical results in Ref. [7]. When fully kinetic electrons are included, TEM instability appears for low η_i. In Fig. 5 it is observed that collisions stabilize the mode and in the particular case where $R/L_n < 3$ the mode is fully suppressed for higher collisionalities, which is in agreement with Ref. [8]. TEM persist depending on whether the value of R/L_n is higher or lower than R/L_{Ti}, i.e. if it is driven predominantly by density or temperature gradients. This result suggests that even in highly collisional plasmas, TEM effects could be of relevance. In the near future, the effects of collisions on ITG and TEM instabilities will be investigated for stellarators.

References

[1] M. Kotschenreuther, Bull. Am. Phys. Soc. **34**, 2107 (1988)

[2] Y. Chen, R.B. White, Phys. Plasmas **4**, 3591 (1997)

[3] S. Brunner, E. Valeo, J.A. Krommes, Phys. Plasmas, **6**, 4504 (1999)

[4] W.X. Wang, N. Nakajima, M. Okamoto, S. Murakami, Plasma Phys. Contr. Fusion, **41**, 1091 (1999)

[5] W.I. van Rij, S.P. Hirshman, Phys. Fluids B **1**, 563 (1989)

[6] Z. Chang, J.D. Callen, Phys. Fluids B **4**, 1182 (1992)

[7] A.M. Dimits, B.I. Cohen, Physical Review E **49**, 709 (1994)

[8] C. Angioni, A.G. Peeters, F. Jenko, T. Dannert, Phys. Plasmas **12**, 112310 (2005)